Vulnerability to Climate Change: Evidence from a Dynamic Factor Model*

Haroon Mumtaz[1] and Fulvia Marotta[2]

[1]Queen Mary University of London
[2]University of Oxford

This version: September 20, 2023.

Abstract

Using a dynamic factor model with stochastic volatility, we examine the synchronization of temperature and precipitation changes across countries and regions. Firstly, the model allows us to quantify the extent of the increase in global temperatures. Secondly, it offers a unique measure of how each country's temperatures align with this common global movement, translating into a robust indicator of exposure to global warming. Our findings reveal that a common factor explains a significant portion of temperature variance globally, with the largest contribution observed in sub-Saharan Africa, Latin America, and Asia. Additionally, the common factor accounts for the increase in temperature levels across these regions. In contrast, precipitation fluctuations exhibit more localized patterns. We find that countries with higher GDP per-capita tend to have lower exposure to global temperature changes.

JEL Classification: Q54, Q58, E32, E37, O13, O44
Keywords: Climate change, Temperatures, Economic Vulnerability, Global Warming, Dynamic factor model.

* *This research was supported by the United Kingdom Foreign, Commonwealth and Development Office through the Climate Compatible Growth Programme and the ClimateWorks Foundation.*

Contents

1 Introduction **3**

2 Empirical Model and Data **5**

2.1 Empirical model 5

2.2 Identification and estimation 6

2.3 Data 7

3 Results **8**

3.1 Factors 8

3.2 Contribution to climate fluctuations 8

3.2.1 Vulnerability and country characteristics 9

3.2.2 Robustness 11

4 Conclusions **12**

A Appendix A: Additional Results and Robustness Checks **23**

A.1 Contribution of regional factor to temperature variance 23

A.2 Robustness checks 23

A.2.1 Fat tails 23

A.3 Two factors 23

A.4 Longer Lags 24

B Gibbs Sampling Algorithm **24**

B.1 Priors 25

1 Introduction

Climate change is increasingly a matter of concern due to its significant impact on macroeconomic fluctuations. Recent papers have emphasized the adverse effects of rising temperatures and climate variability on real economic activity, particularly in low-income countries (Alessandri and Mumtaz (2022), Dell *et al.* (2012)). However, the uncertainty surrounding the pace of climate change and its potential long-term impacts poses challenges for researchers, making it difficult to draw definitive conclusions about its effects on the economy. Our work closely aligns with this growing literature that aims to test these channels and their macroeconomic consequences.

Regarding the impacts of global warming, specifically the gradual rise in average temperatures, the literature consistently indicates that such increases have adverse effects on the economy. However, it is important to note that the extent of these effects varies significantly across countries due to their unique characteristics and vulnerabilities (Burke and Tanutama (2019)). Extreme temperatures have been found to reduce output (Burke and Hsiang (2015)), labor productivity (Donadelli *et al.* (2017)), agricultural production (Winne and Peersman (2019)), food security (Bandara and Cai (2014), Schaub and Finger (2020)), and overall economic growth (Cipollini and Parla (2023), Kim *et al.* (2021), Kahn *et al.* (2021), Carleton and Hsiang (2016),Deryugina and Hsiang (2014)). The impact of physical risks deriving from global warming or extreme weather events on prices and inflation is found to vary substantially by type, severity, location, and sector of the economy (Ciccarelli *et al.* (2023), Canova and Pappa (2021), Baldauf and Lorenzo Garlappi (2020), Parker (2018), Heinen *et al.* (2018), Cavallo *et al.* (2014),). Existing evidence predominantly focuses on the supply-side effects of climate change on the economy, while research on demand-side threats is limited. These threats result from disruptions to income, consumption patterns, investments, exports, and changes in consumer behavior, influenced by migration and climate awareness. Climate change intensifies natural disasters and environmental degradation, leading to premature deaths, injuries, displacements, and adverse impacts on well-being and welfare (Ciccarelli and Marotta (2021)).

Given the mounting evidence studying the links between climate change and the economy, our paper aims to develop an empirical framework for assessing the synchronization of movements of temperatures and precipitation's patterns across countries and regions for the past 120 years.

More in detail, in this study we employ a factor model with stochastic volatility to analyse the extent to which changes in temperature and precipitations exhibit common patterns across various world regions. However, rather than focusing solely on the synchronicity

of temperatures and precipitation, our novel approach isolates the common movement in these climate variables that is shared by all countries in the sample. This framework provides two essential insights: firstly, it allows us to quantify the extent of the increase in global temperatures, providing a comprehensive measure of the global warming phenomenon. Secondly, it offers a unique measure of how each country's temperatures align with this common global movement, which translates into a robust indicator of exposure to global warming. This dual aspect of our framework enables a more nuanced understanding of countries' vulnerability to climate risks and provides valuable information for policymakers in crafting effective adaptation and mitigation strategies.

Measuring countries' vulnerability to global warming holds significant importance for addressing the challenges posed by climate change. It allows for the identification of regions and nations at higher risk of adverse impacts, such as extreme temperatures and natural disasters, enabling policymakers to prioritize resources and implement targeted measures to build resilience. Understanding vulnerability provides insights into the potential economic consequences of global warming, helping countries prepare for challenges like reduced agricultural productivity, increased healthcare costs, and disruptions to infrastructure. Additionally, it aids in international climate negotiations and the allocation of climate finance, ensuring equitable support for highly vulnerable nations. By tailoring climate policies to specific needs, measuring vulnerability contributes to sustainable development goals and fosters climate resilience, ensuring no one is left behind in the face of climate change.

Our findings reveal that a common factor explains a significant portion of the temperature variance in major regions globally, with the largest contribution observed in sub-Saharan Africa, Latin America, and Asia. Furthermore, this common factor ac- counts for the overall increase in temperature levels across these regions. We also observe that countries more susceptible to common temperature movements tend to have lower GDP per capita, a higher share of agriculture and to a lower extent industry in GDP, and higher average temperatures. On the other hand, the co-movement of precipitation is more localized and less evident.

Moreover, to track changes in climate conditions over time and regions, macroeconomic studies often make use of average temperatures, temperature anomalies or composite indexes using both temperatures and precipitations. However, these measures may face challenges in discerning the specific effects of climate change from other factors. In contrast, our proposed measure offers a more robust isolation of global warming's impact on temperature and precipitation changes, providing a comprehensive assessment of coun-

tries' vulnerability to climate risks. Furthermore, our exposure measure is aligned with the ND Gain Index[1], showing a positive correlation with their vulnerability index and a negative correlation with their readiness index, highlighting its relevance in climate resilience policy decision-making.

The rest of the paper is structured as follows: Section 2 of this paper provides a detailed description of the model used and the dataset employed in our analysis. In Section 3, we present and discuss the results obtained from our empirical investigation.

2 Empirical Model and Data

2.1 Empirical model

We assume that the average annual temperature (T_{it}) and average annual precipitation (P_{it}) data are described by unobserved components that are common across countries or regions. We model these features using a dynamic factor model that allows for heteroscedastic disturbances.

The series in our panel are described by the following observation equation:

$$\begin{pmatrix} T_{it} \\ P_{it} \end{pmatrix} = \begin{pmatrix} B_i^W & 0 \\ 0 & \beta_i^W \end{pmatrix} \begin{pmatrix} F_t^W \\ f_t^W \end{pmatrix} + \begin{pmatrix} B_i^R & 0 \\ 0 & \beta_i^R \end{pmatrix} \begin{pmatrix} F_t^R \\ f_t^R \end{pmatrix} + \begin{pmatrix} v_{it} \\ e_{it} \end{pmatrix} \tag{1}$$

where $\underbrace{F_t^W}_{K\times 1}$ and $\underbrace{f_t^W}_{K\times 1}$ denotes a set of K factors that are common across all countries with associated factor loadings $\underbrace{B_i^W}_{1\times K}$ and $\underbrace{\beta_i^W}_{1\times K}$. F_t^W represent the 'world' factor for temperature while f_t^W is the counterpart for precipitation. Region-specific factors are denoted by the matrices $\underbrace{F_t^R}_{K\times 1}$ and $\underbrace{f_t^R}_{K\times 1}$ with factor loadings denoted by the $1 \times K$ vectors B_i^R and β_i^R. These factors are distinct from the world factors as they only load on the data for the rth region. The idiosyncratic components in T_{it} (P_{it}) is captured by v_{it} (e_{it}) for $i = 1, 2, ..., M$. The world and regional factors are assumed to follow a VAR(2) process:

$$Z_t = c + \sum_{j=1}^{2} b_j Z_{t-j} + E_t \tag{2}$$

[1]The ND-GAIN Index is an initiative developed by the Notre Dame Global Adaptation Institute (GAIN) that assesses and ranks countries based on their vulnerability to climate change and their readiness to adapt and respond to its impacts.

where $\underbrace{Z_t}_{N\times 1} = \left(F_t^W, f_t^W, F_t^R, f_t^R\right)$ The idiosyncratic components are assumed to follow AR(1) processes [2]:

$$\begin{pmatrix} v_{it} \\ e_{it} \end{pmatrix} = \begin{pmatrix} \rho_i & 0 \\ 0 & p_i \end{pmatrix} \begin{pmatrix} v_{it-1} \\ e_{it-1} \end{pmatrix} + \begin{pmatrix} \varepsilon_{it} \\ \eta_{it} \end{pmatrix} \tag{3}$$

We allow the disturbances of the model to be heteroscedastic. The shocks $\Upsilon_{it} = \begin{pmatrix} \varepsilon_{it} \\ \eta_{it} \end{pmatrix}$ are assumed to have the following distribution:$\Upsilon_{it} \sim N\left(0, \sigma_{it}\right)$. The variance σ_{it}^2 is allowed to evolve over time:

$$\ln \sigma_{it}^2 = \tilde{c}_i + \tilde{d}_i \ln \sigma_{it-1}^2 + g_i v_{it} \tag{4}$$

As discussed below, the covariance matrix of E_t is assumed to be diagonal for the purpose of identification. Each element of E_t is distributed normally: $E_{kt} \sim N\left(0, h_{kt}\right)$ for $k = 1, .., N$. The stochastic volatilities h_{kt} evolve as AR processes [3]:

$$\ln h_{kt} = \bar{c}_k + \bar{D}_k \ln h_{kt-1} + d_k u_{kt} \tag{5}$$

2.2 Identification and estimation

Without additional assumptions, the model in equations 1 and 2 suffers from rotational indeterminancy. To identify the factors and factor loadings, we follow Bai and Wang (2015) and impose the following identifying restrictions: (i) The covariance matrix of E_t is assumed to be diagonal. (ii) The top $K \times K$ block of the factor loading matrices β and B are assumed to be lower triangular with ones on the main diagonal.

As described in detail in the technical appendix, the model is estimated using a Gibbs sampling algorithm. The algorithm samples from the following conditional posterior distributions in each iteration:

1. Factors: Conditional on the stochastic volatilities, the parameters of the observation and transition equations, the model has a linear, Gaussian state-space representation. The algorithm of Carter and Kohn (2004) is used to sample from the conditional posterior distribution of the factors.

2. Stochastic volatilities: The stochastic volatilites σ_{jt}^2 and h_{kt} are drawn from their

[2] As shown in the Appendix, our results are not sensitive to using alternative lag lengths.

[3] We show in the technical appendix that an extended version of the model that features non-normal disturbances produces similar results to the benchmark case.

conditional posteriors using a particle Gibbs sampler with ancestor sampling (see Lindsten *et al.* (2014)).

3. Factor loadings: The observation equation is a Bayesian regression with known form of heteroscedasticity. After a GLS transformation, the conditional posterior is normal with known moments.

4. Parameters of the transition equations. Conditional on the factors and the idiosyncratic components, the model collapses to the VAR in equations 2 and the AR models in equation 3. Conditional on the time-varying volatility of the residuals, the conditional posteriors of the coefficients are normal. The transition equations 4 and 5 are Bayesian linear regressions and the conditional posterior of the coefficients and the error variance is normal and inverse Gamma, respectively.

We use 21,000 iterations saving every 5th of the last 20,000 for inference. We use the saved parameter draws to calculate the contributions of the world and country factors to the level and variance of the climate variables. The decomposition of the level follows from the observation equation 1 where the contributions from the world and regional factors are provided by the 'fitted values' $\hat{\Phi}_i^W \left(\hat{F}_t^W\right)$ and $\hat{\Phi}_i^R \left(\hat{F}_t^R\right)$ where $\Phi_i^J = \begin{pmatrix} B_i^J & 0 \\ 0 & \beta_i^J \end{pmatrix}$ and $F_t^J = \begin{pmatrix} F_t^J \\ f_t^J \end{pmatrix}$ for $J = W, R$. The variance of X_{it} is defined as :

$$var\left(X_{it}\right) = \left(\hat{\Phi}_i^W\right) \hat{\Theta}^W \left(\hat{\Phi}_i^W\right)' + \left(\hat{\Phi}_i^R\right) \hat{\Theta}^R \left(\hat{\Phi}_i^R\right)' + var\left(V_{it}\right) \tag{6}$$

where $\Theta^J = diag\left(var\left(\hat{F}_t^J\right)\right)$ and $V_{it} = \begin{pmatrix} v_{it} \\ e_{it} \end{pmatrix}$. The variance terms Θ^J on the RHS of equation 6 can be calculated by applying the standard VAR formula for the unconditional variance at each point in time, while $var\left(V_{it}\right) = \frac{\left(\sigma_{it}^2\right)}{1-\rho_i^2}$.

2.3 Data

For each country, we collect data on temperatures and precipitations. The data is obtained from the University of East Anglia Climate Research Unit's (CRU) high-resolution data sets. The data set includes annual series, spatially averaged over individual countries. Temperatures are expressed in Centigrade while precipitations in millimetres per year. Overall our sample includes 166 countries. The time series spans from 1900 to 2020. We use the first 20 years of the sample to calibrate the priors and obtain initial values.

3 Results

3.1 Factors

Figure 1 shows the posterior estimates of the two world factors. The temperature factor fluctuates at about $18°C$ until 1980. However, the temperature factor shows a marked increase after this date reaching $19°C$ at the end of the sample. This result provides strong evidence that an increase in temperatures is a global phenomenon. In contrast to the temperature factor, the world precipitation factor shows a modest decline in the post-1970 period.

Figures 2 shows the evolution of average temperatures in the different regions along with the 'fitted values' $\hat{X}_{it}^W = B_i^W F_T^W$ and $\hat{X}_{it}^R = B_i^R F_T^R$, respectively. Average temperatures have increased in all regions and the world factor accounts for the bulk of this increase. In Sub-Saharan Africa, Latin America and Asia, the predicted temperature due to the world factor tracks the actual temperature almost exactly and the prediction due to the regional factor is largely flat. For the remaining regions, the regional factors capture some of the large movements in temperature but the post-1980 warming is explained largely by the world factor.

There is some evidence that higher frequency movements in precipitation in the Middle East and North Africa, Europe, North America, and Asia are region specific with the predicted value due to the regional factor moving in line with the actual data. It is interesting to note that the global factor is important for Sub-Saharan Africa and explains the sharp decline in precipitation after the mid-1970s.

3.2 Contribution to climate fluctuations

As noted above, the model allows a decomposition of the variance of temperature and precipitation into contributions from the world and regional factors. The contributions of the world factor to temperature volatility, for example, provide a measure of exposure and vulnerability of countries to the rise in temperature documented above.

The heat map in Figure 4 shows that the contribution of the world factor to temperature fluctuations is large with a cross-country average of 52 percent. The role of the world factor is especially important in Sub-Saharan Africa, Latin America and Asia with impact of the world factor exceeding 80 percent– the top five countries in terms of contributions of this factor are Saint Vincent and the Grenadines, Venezuela, Trinidad and Tobago, Sri Lanka and Tanzania. In contrast, countries such as Sweden, Finland and Norway are largely unaffected by the common developments in temperature. It is interesting to

note that some large industrial countries are highly vulnerable to common temperature developments. For example, the contribution of this factor to temperature fluctuations in the United States and China is estimated to be 60 percent and 66 percent, respectively. [4] Figure A.1 in Appendix A shows that the regional factor makes a modest contribution to temperature variance, explaining, on average, 20 percent of fluctuations. This factor is important for some countries in Western and Eastern Europe– it contributes about 60 percent to the volatility of temperature in Denmark, Slovakia, Poland and the Netherlands. The contribution of the global factor to precipitation volatility is small (8 percent on average), indicating that there is limited co-movement in this variable over time. The effect of the factor is largest in Sub-Saharan Africa and Latin-America and the Caribbean. However, in absolute terms, the contribution of this factor remains small. The regional factor is somewhat more important for precipitation (see Figure A.2 in the appendix) with an average contribution of 16 percent. Countries such as Belgium, Netherlands, Luxembourg and Germany in Western Europe and Jordan and Israel in the Middle East are highly exposed to this factor with 70 to 80 percent of fluctuations in precipitation explained by regional co-movement.

3.2.1 Vulnerability and country characteristics

Why are some countries more exposed to the global temperature factor? We provide some tentative results on this issue by performing the following correlation analysis to explore the relationships between economic, energy and development indicators and their associations with the exposure to the global temperature factor.[5]

The findings, described by the heat map in Figure 6 reveal important insights into these associations. Overall, the results indicate that countries with higher GDP per capita tend to have lower exposure to global temperature changes. A positive significant correlation is observed between the share of agriculture (0.32) over GDP and the contribution of the world temperature factor to temperature suggesting that countries with a larger propor-

[4] The contributions of the world factor is significantly and positively correlated with the University of Notre Dame ND-GAIN index of climate vulnerability and negatively correlated with their readiness index. The correlation coefficient between the two is 0.39 and -0.43 for vulnerability and readiness respectively with p-values close to zero.

[5] The variables included in the analysis are: GDP per capita, Share of agriculture, industry, service and manufacturing in GDP, Energy use (kg of oil equivalent per capita), CO2 emission intensity (kg per 2015 US$ of GDP), Fossil fuel energy consumption (% of total), Life expectancy (years), School enrollment (secondary, % children of school age), Urban population (% of total population), the University of Notre Dame index of climate readiness, the University of Notre Dame index of climate vulnerability, Average temperature and Average precipitation. Indicators are averaged over the available time-series 1950-2006. The variables used in this analysis were obtained from the World Bank Development Indicators database.

tion of their economies in this sector may experience slightly higher exposure to global temperature changes.

The observed correlation can be attributed to several factors. Firstly, countries with higher GDP per capita often have more resources and technological capabilities to adapt and mitigate the effects of climate change. They may have better infrastructure, healthcare systems, and access to resources that enable them to implement effective measures to cope with rising temperatures. These countries are more likely to invest in climate change adaptation strategies, such as improved water management systems, energy-efficient technologies, and early warning systems, which can help mitigate the adverse impacts of temperature changes.

Secondly, higher GDP per capita is often associated with greater economic diversification and a lower dependency on climate-sensitive sectors, such as agriculture. Countries with a larger share of their economies in agriculture tend to be more susceptible to climate variations, as agricultural productivity is highly dependent on weather conditions. In contrast, countries with more diversified economies, including a higher share of services, are less reliant on climate-sensitive sectors and therefore exhibit lower exposure to global temperature changes. It is important to note that while the correlation between GDP per capita and exposure to global temperature changes is observed, it does not necessarily imply causation. Other factors, such as historical development trajectories, governance structures, and geographical location, may also play a role in shaping a country's vulnerability and exposure to climate change. Additionally, the specific policies and measures implemented by each country to address climate change can further influence their exposure levels.

Moreover, higher energy consumption per capita is associated with lower exposure to global temperature changes, as indicated by the negative correlation (-0.18) between energy use (kg of oil equivalent per capita) and the exposure to the global temperature factor. Furthermore, lower emissions intensity (-0.13) and a lower proportion of energy derived from fossil fuels (-0.23) are correlated with slightly higher exposure to global temperature changes, as indicated by the negative correlations between emissions intensity and fossil fuel intensity with exposure to the global temperature factor. Higher energy consumption per capita is associated with lower exposure to global temperature changes because countries with higher energy consumption tend to have more developed and industrialized economies. These countries typically have greater resources and capabilities to invest in technologies and infrastructure that can help mitigate the effects of rising temperatures. They may have access to cleaner and more efficient energy sources, advanced manufacturing processes, and better energy management practices, which can reduce their overall

vulnerability to global temperature changes.
Socioeconomic factors also play a role, with countries having higher life expectancy (-0.39) and higher secondary school enrollment rates (-0.44) being associated with lower exposure to global temperature changes. Additionally, it is also negatively correlated with the urbanization rate (-0.40), suggesting that countries with higher urbanization rates tend to have lower exposure to global temperature changes.
Two additional variables, readiness and vulnerability demonstrate significant associations with the exposure to the global temperature factor. Readiness exhibits a negative correlation (-0.43), indicating that countries with higher readiness levels tend to have lower exposure to global temperature changes. This suggests that countries with well-developed strategies, infrastructure, and resources for addressing climate change may be better equipped to mitigate the impacts of rising temperatures. On the other hand, vulnerability shows a positive correlation (0.39) suggesting that countries with higher vulnerability levels, encompassing factors such as exposure, sensitivity, and adaptive capacity, may experience greater exposure to global temperature changes and associated risks. Furthermore, results confirm that higher average temperatures and precipitations are associated with increased exposure to global temperature changes. These findings provide valuable insights into the relationships between these country characteristics and the distribution of countries' exposure to the global temperature factor. However, it is important to note that correlation does not imply causation. Further analysis, such as regression modeling, is necessary to establish the significance and causal relationships between these variables and the exposure to global temperature changes.

3.2.2 Robustness

We carry out three robustness checks that are described in detail in Appendix A.

1. Fat tails: The benchmark model assumes Gaussian disturbances. First, we relax this assumption and model the idiosyncratic residuals and shocks to the transition equation for the factors using a Student-t distribution with 10 degrees of freedom. This version of the model produces factors and variance decomposition that is similar to benchmark.

2. Two factors: We extend the model and increase in the number of world and regional factors to 2. As shown in Appendix A the first temperature and precipitation factors are similar to the benchmark case. Our key result regarding the importance of the world factor for temperature volatility is preserved. However, as the additional

common factors capture higher-frequency fluctuations in the climate data, the share of variation of temperature explained by the global factors is higher than in the benchmark case.

3. Longer lags: The appendix also shows that a version of the benchmark model with additional lags produces results that are very similar to the benchmark case.

4 Conclusions

In this study, we contribute to the growing literature exploring the link between climate change and macroeconomic fluctuations by examining the synchronization of temperature and precipitation changes across countries and regions. Our empirical analysis, based on a factor model with stochastic volatility, has yielded several key findings. First, we observed a significant increase in global temperatures after 1980, indicating that rising temperatures are indeed a global phenomenon. The world factor accounted for the majority of this temperature increase, particularly in sub-Saharan Africa, Latin America, and Asia. In these regions, the predicted temperature due to the world factor closely tracked the actual temperature, while the regional factor had a minimal impact. In other regions, the regional factors captured some temperature movements, but the post-1980 warming was primarily explained by the world factor. On the other hand, precipitation fluctuations exhibited more localized patterns, with limited evidence of co-movement across regions over time. However, the global factor did play a role in explaining the sharp decline in precipitation after the mid-1970s in Sub-Saharan Africa. Overall, the contribution of the global factor to precipitation volatility was relatively small compared to that of temperature.

The decomposition of temperature and precipitation variances allowed us to assess the contribution of the world and regional factors to climate fluctuations. We found that the world factor accounted for a significant proportion (52 %) of temperature fluctuations globally, with higher contributions in regions such as Sub-Saharan Africa, Latin America, and Asia. Countries with lower GDP per capita and a higher share of agriculture and to a lower extent industry in their economies tended to exhibit greater exposure to global temperature changes. Additionally, higher energy consumption per capita was associated with lower exposure to global temperature fluctuations, while lower emissions intensity and a lower proportion of energy derived from fossil fuels were correlated with slightly higher exposure.

Socioeconomic factors also played a role, with countries experiencing lower exposure to global temperature changes having higher life expectancy, higher secondary school en-

rollment rates, and lower urbanization rates. Furthermore, countries with higher readiness levels demonstrated lower exposure, indicating that well-developed strategies and resources for addressing climate change can help mitigate the impacts of rising temperatures. Conversely, countries with higher vulnerability levels showed greater exposure to global temperature changes, emphasizing the need for adaptive capacity and resilience-building measures.

In conclusion, our study highlights the global nature of temperature increases and the varying degrees of synchronization in precipitation fluctuations across regions. The findings provide valuable insights into the vulnerability and exposure of countries to climate change, helping policymakers better understand the implications of climate risks on economic stability. Further research, including regression modeling and in-depth analysis of causality, is needed to deepen our understanding of the complex relationships between climate variables and macroeconomic outcomes. Ultimately, addressing climate change and building resilience will require concerted efforts at both the global and regional levels, with targeted strategies tailored to the specific challenges faced by different countries and regions.

References

Alessandri, Piergiorgio and Haroon Mumtaz, 2022, The macroeconomic cost of climate volatility, *BCAM Working Papers 2202*, Birkbeck Centre for Applied Macroeconomics.

Bai, Jushan and Peng Wang, 2015, Identification and Bayesian Estimation of Dynamic Factor Models, *Journal of Business & Economic Statistics* **33**(2), 221–240.

Baldauf, Markus and Constantine Yannelis Lorenzo Garlappi, 2020, Does Climate Change Affect Real Estate Prices? Only If You Believe In It, *The Review of Financial Studies* **33**(3), 1256–1295.

Bandara, Jayatilleke S. and Yiyong Cai, 2014, The impact of climate change on food crop productivity, food prices and food security in South Asia, *Economic Analysis and Policy* **44**(4), 451 – 465.

Bańbura, Marta, Domenico Giannone and Lucrezia Reichlin, 2010, Large Bayesian vector auto regressions, *Journal of Applied Econometrics* **25**(1), 71–92.

Burke, Marshall and Solomon Hsiang, 2015, Global non-linear effect of temperature on economic production, *Nature* **527**.

Burke, Marshall and Vincent Tanutama, 2019, Climatic Constraints on Aggregate Economic Output, *Working Paper 25779*, National Bureau of Economic Research.

Canova, Fabio and Evi Pappa, 2021, Costly disasters and the role of fiscal policy, *mimeo*.

Carleton, Tamma A and Solomon M Hsiang, 2016, Social and economic impacts of climate, *Science* **353**(6304).

Carriero, Andrea, Joshua Chan, Todd E. Clark and Massimiliano Marcellino, 2022, Corrigendum to "Large Bayesian vector autoregressions with stochastic volatility and non-conjugate priors" [J. Econometrics 212 (1) (2019) 137–154], *Journal of Econometrics* **227**(2), 506–512.

Carter, C and P Kohn, 2004, On Gibbs sampling for state space models, *Biometrika* **81**, 541–553.

Cavallo, Alberto, Eduardo Cavallo and Roberto Rigobon, 2014, Prices and Supply Disruptions during Natural Disasters, *Review of Income and Wealth* **60**(S2), S449–S471.

Ciccarelli, Matteo, Friderike Kuik and Catalina Martínez Hernández, 2023, The asymmetric effects of weather shocks on euro area inflation.

Ciccarelli, Matteo and Fulvia Marotta, 2021, Demand or supply? An empirical exploration of the effects of climate change on the macroeconomy, *Working Paper Series 2608*, European Central Bank.

Cipollini, Andrea and Fabio Parla, 2023, Temperature and Growth: a Panel Mixed Frequency VAR Analysis using NUTS2 data, *RECENT WORKING PAPER SERIES, Dipartimento di Economia Marco Biagi-Università di Modena e Reggio Emilia* .

Dell, Melissa, Benjamin F. Jones and Benjamin A. Olken, 2012, Temperature Shocks and Economic Growth: Evidence from the Last Half Century, *American Economic Journal: Macroeconomics* **4**(3), 66–95.

Deryugina, Tatyana and Solomon M Hsiang, 2014, Does the Environment Still Matter? Daily Temperature and Income in the United States, *Working Paper 20750*, National Bureau of Economic Research.

Donadelli, M., M. Jüppner, M. Riedel and C. Schlag, 2017, Temperature shocks and welfare costs, *Journal of Economic Dynamics and Control* **82**(C), 331–355.

Geweke, J., 1993, Bayesian Treatment of the Independent Student-t Linear Model, *Journal of Applied Econometrics* **8**, S19–S40.

Heinen, A., J. Khadan and E. Strobl, 2018, The price impact of extreme weather in developing countries, *The Economic Journal* **1258**.

Kahn, Matthew E, Kamiar Mohaddes, Ryan NC Ng, M Hashem Pesaran, Mehdi Raissi and Jui-Chung Yang, 2021, Long-term macroeconomic effects of climate change: A cross-country analysis, *Energy Economics* **104**, 105624.

Kim, Hee Soo, Christian Matthes and Toan Phan, 2021, Extreme weather and the macroeconomy, *Available at SSRN 3918533* .

Koop, Gary, 2003, *Bayesian Econometrics*, Wiley.

Lindsten, Fredrik, Michael I. Jordan and Thomas B. Schön, 2014, Particle Gibbs with Ancestor Sampling, *Journal of Machine Learning Research* **15**, 2145–2184.

Parker, Miles, 2018, The Impact of Disasters on Inflation, *Economics of Disasters and Climate Change* **2**(1), 21–48.

Schaub, Sergei and Robert Finger, 2020, Effects of drought on hay and feed grain prices, *Environmental Research Letters* **15**(3), 034014.

Winne, Jasmien De and Gert Peersman, 2019, The Impact of Food Prices on Conflict Revisited, *Working Papers of Faculty of Economics and Business Administration, Ghent University, Belgium 19/979*, Ghent University, Faculty of Economics and Business Administration.

Figure 1: World factors

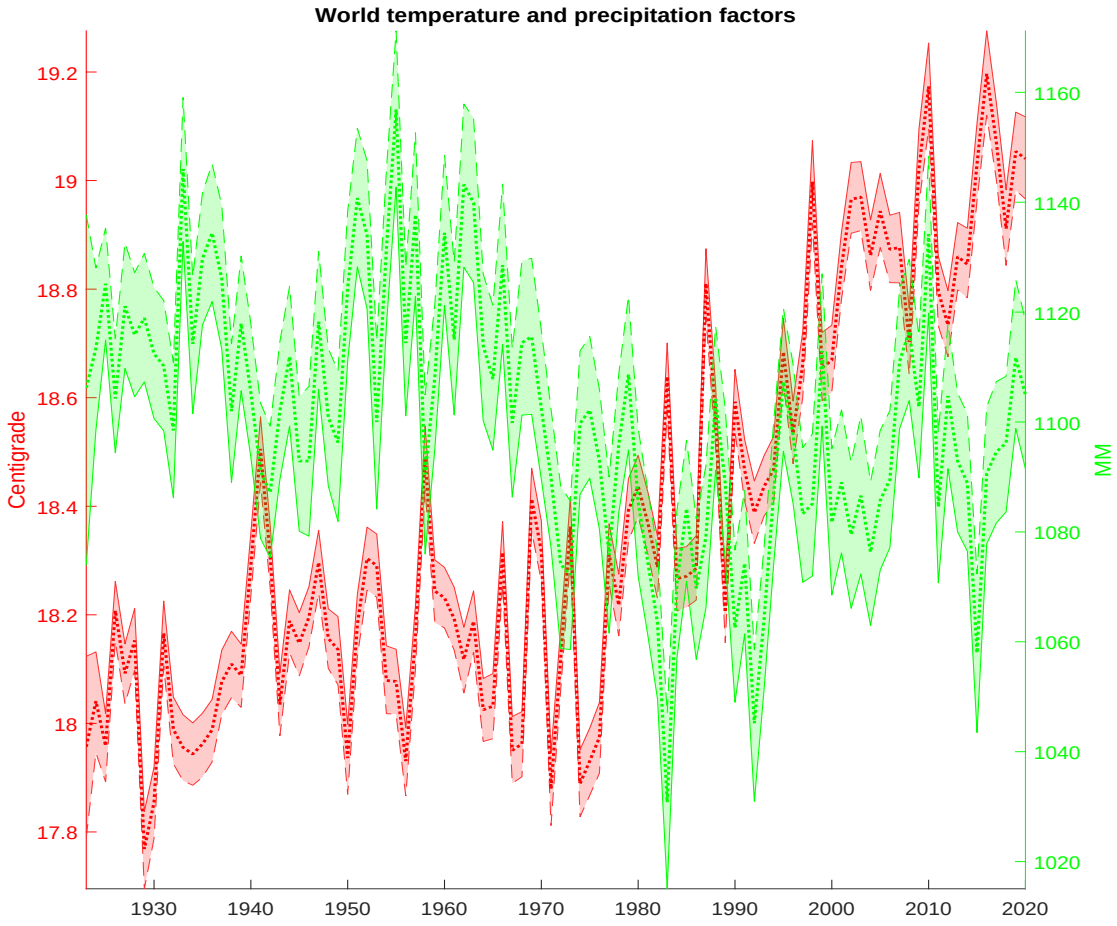

Estimated world factors for temperature (left axis) and precipitation (right axis). The shaded areas represent the 95 percent error band

Figure 2: World and regional factors for temperature

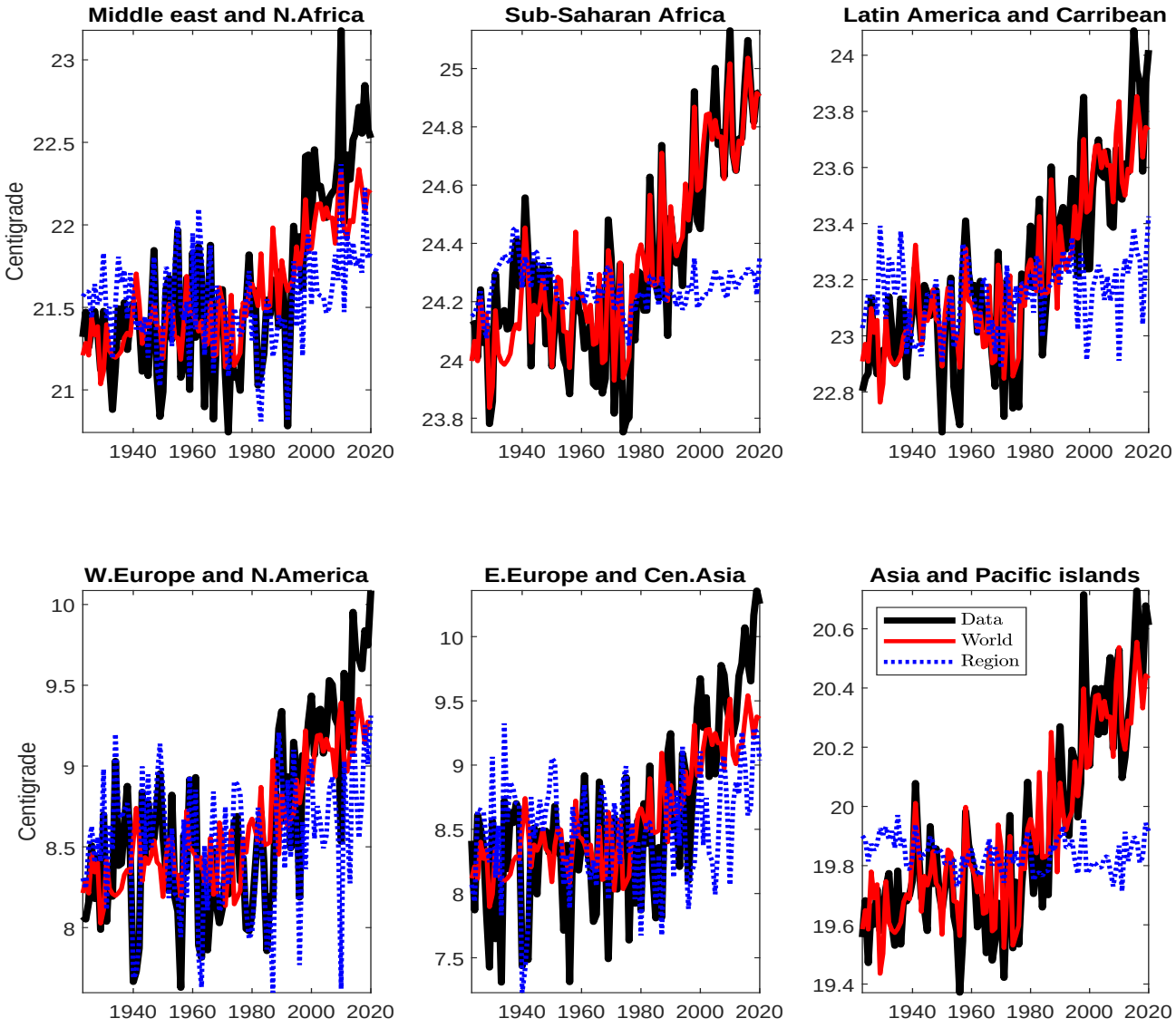

Estimated world and regional factors for temperature and average regional temperature

Figure 3: World and regional factors for precipitation

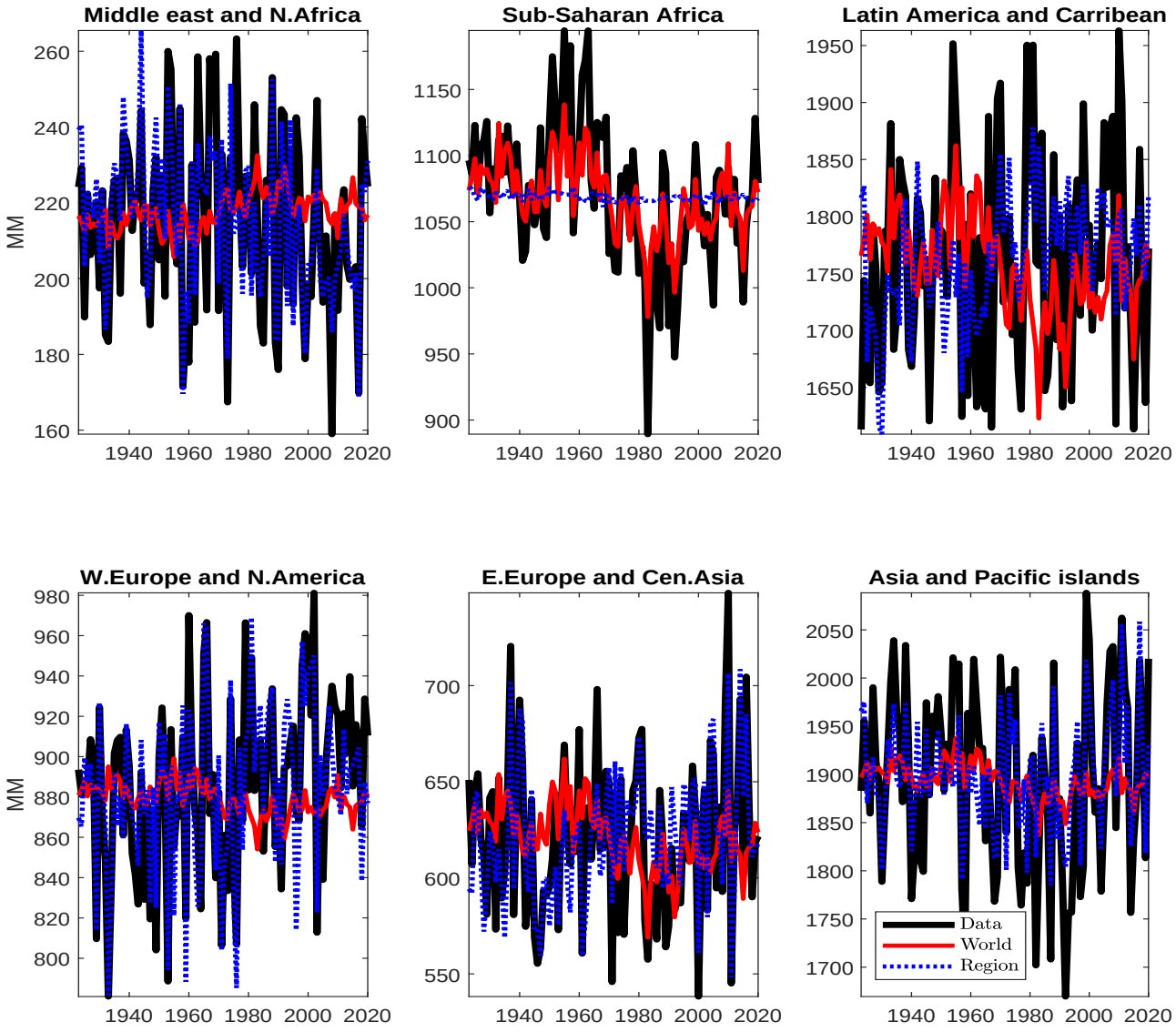

Estimated world and regional factors for precipitation and average regional precipitation

Figure 4: Contribution of the world factor to temperature volatility. Average across time

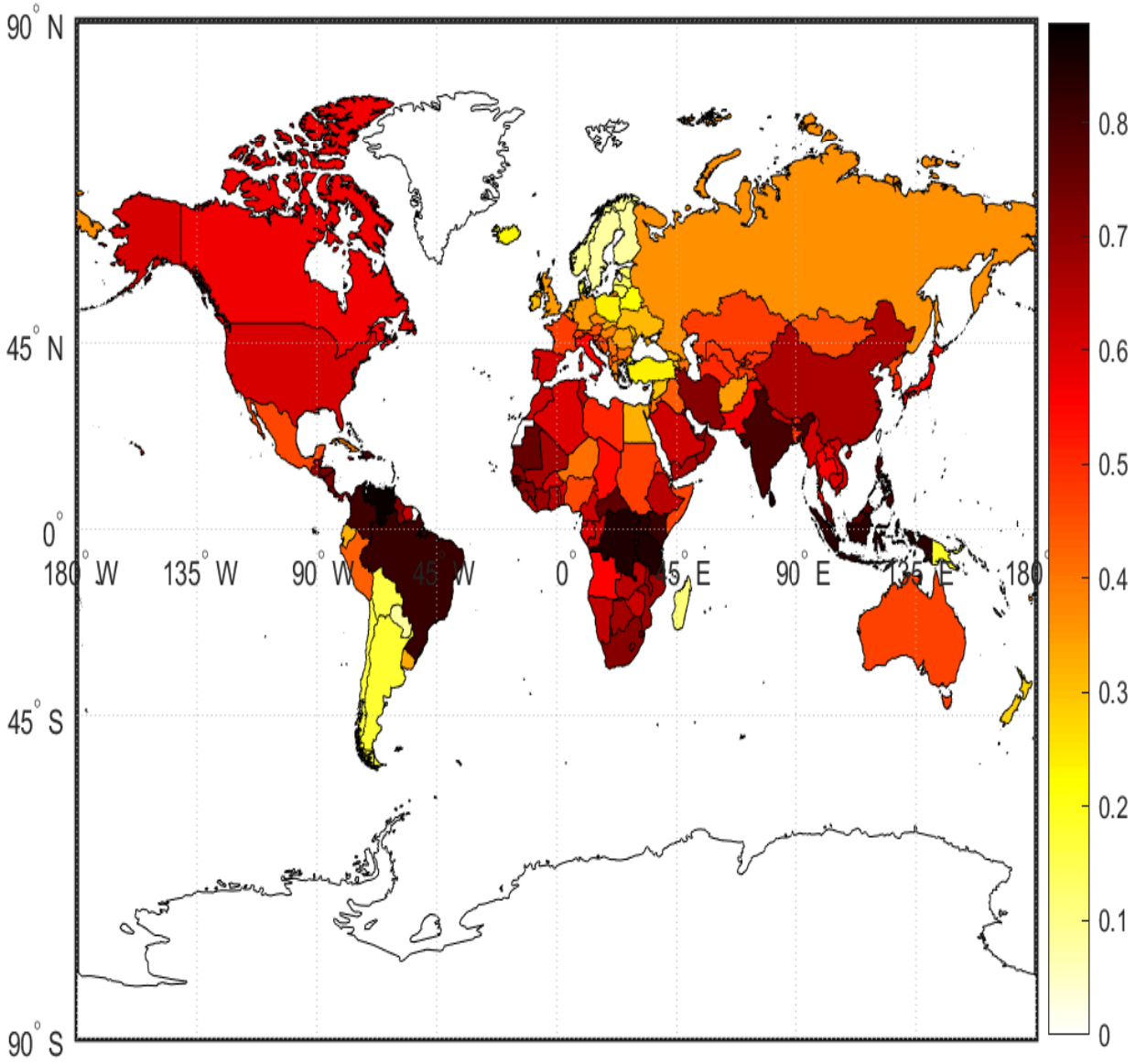

Darker colours the heat map indicates a larger contribution

Figure 5: Contribution of the world factor to precipitation volatility. Average across time.

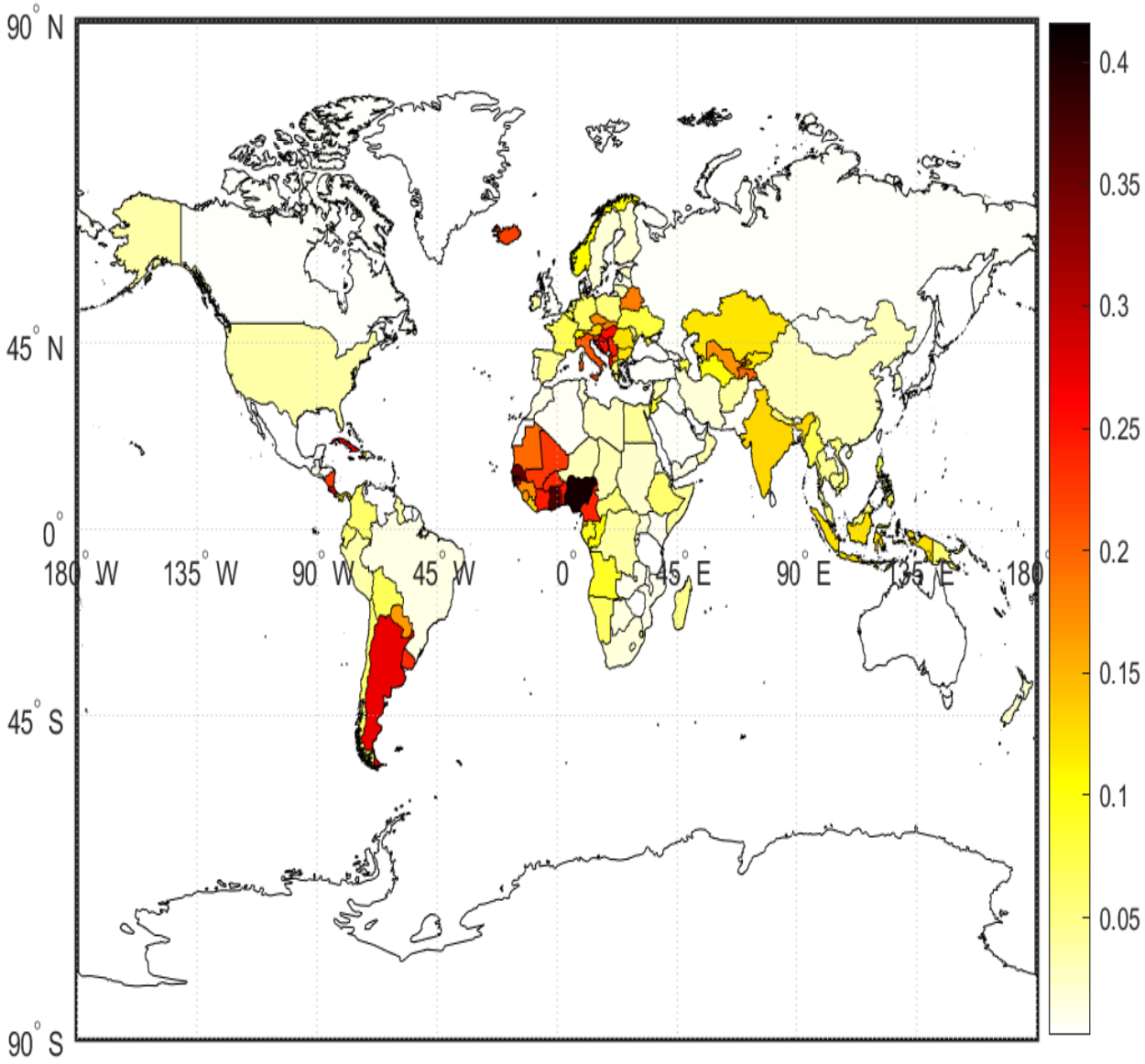

Darker colours the heat map indicates a larger contribution

Figure 6: Vulnerability and country characteristics: correlation heat map

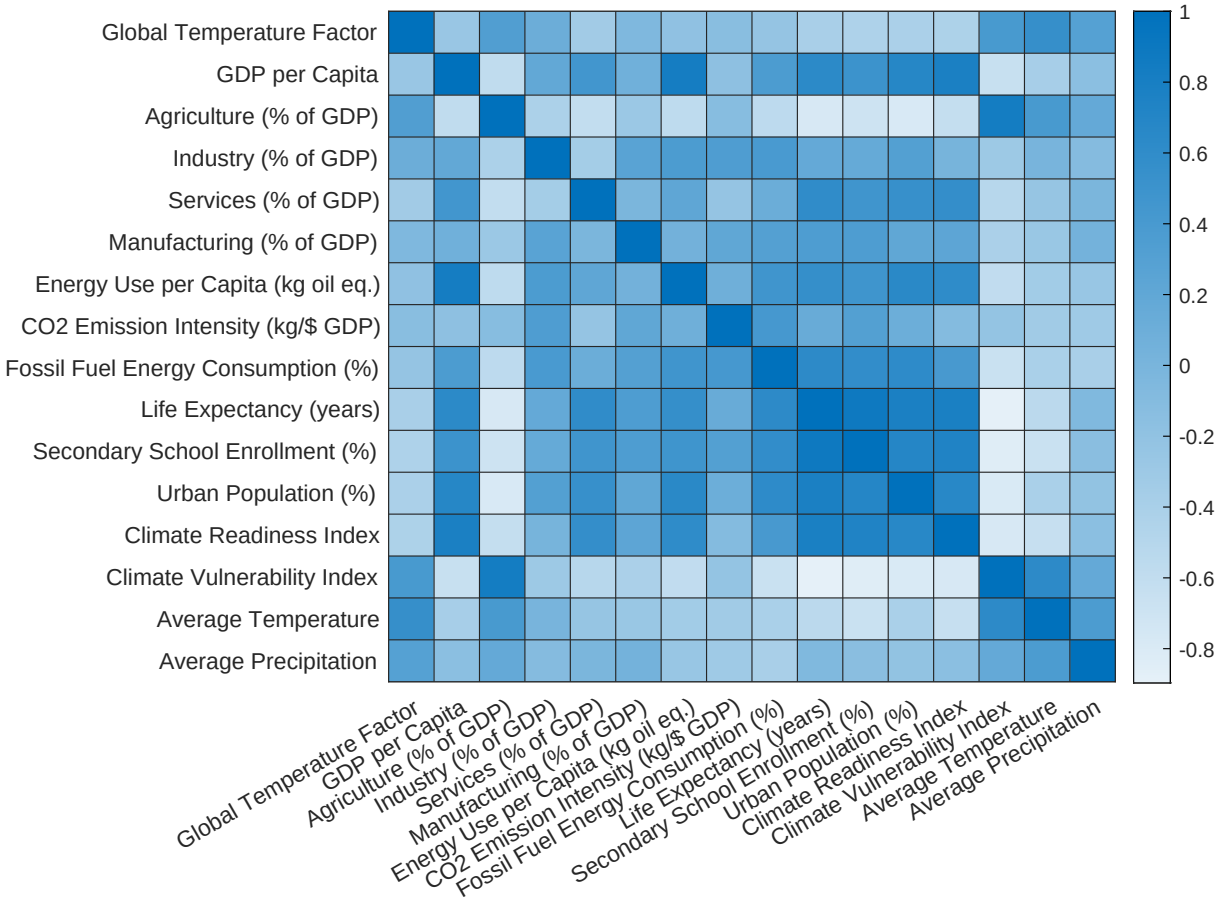

A Appendix A: Additional Results and Robustness Checks

A.1 Contribution of regional factor to temperature variance

Figure A.1 shows the contribution of the regional factor to temperature volatility while figure A.2 shows the contribution of the regional factor to precipitation volatility. See main text for details.

A.2 Robustness checks

A.2.1 Fat tails

First, we relax the assumption of normal disturbances in the benchmark model. The idiosyncratic components are defined as $\Upsilon_{it} \sim N\left(0, \frac{\sigma_{it}^2}{\lambda_{it}}\right)$. The variance σ_{it}^2 is allowed to evolve slowly over time and follows an AR model as described above. Higher frequency movements in volatility are captured by $\frac{1}{\lambda_{it}}$ that is independent over time. Following Geweke (1993), we assume a Gamma prior for λ_{it} of the form $p(\lambda_i) = \prod_{i=1}^{T} \Gamma(1, v_i)$, where $\Gamma(a, b)$ is the gamma density with mean a and degrees of freedom b. This leads to a scale mixture of normal distributions for Υ_{it} implying that these residuals follow a student's T density with degrees of freedom v_i and variance σ_{it}^2. The same specification is assumed for the shocks to the transition equation 2. As discussed below, the covariance matrix of E_t is assumed to be diagonal for the purpose of identification. Each element of E_t is distributed normally: $E_{kt} \tilde{} N\left(0, \frac{h_{kt}}{\gamma_{kt}}\right)$ for $k = 1, .., N$. The weights $\frac{1}{\gamma_{kt}}$ capture high frequency movements in volatility. As above, we assume a Gamma prior for γ_{kt}: $p(\gamma_k) = \prod_{i=1}^{T} \Gamma(1, v_j)$. The degrees of freedom parameters ν are set to 10 implying tails that are fatter than the normal density. We add steps in the Gibbs sampler to draw λ_{it} and γ_{kt}. The conditional posterior distribution for this parameter is described in Koop (2003). Figure A.3 shows that the estimated factors are close to the benchmark case. In additionn, the variance decomposition has a pattern that is similar to benchmark with the world factor playing a major role in explaining temperature fluctuations.

A.3 Two factors

We extend the benchmark model and add two world and regional factors. The top panels of figure A.4 display the estimated world factors. The first temperature factor displays

the temporal pattern seen in the benchmark case with a sharp increase evident in the post-1980 period. Similarly, the first precipitation factor displays a decline after the mid-1970s. The second temperature and precipitation factors are more volatile and do not have a clear interpretation. In terms of the variance decomposition, the role of the world temperature factors is magnified in this extended model as some of the higher frequency movements in temperature are also explained by the second factor. As in the benchmark case, the regional factor remains important for precipitation volatility.

A.4 Longer Lags

We re-estimate the model using 4 lags in the transition equation for the factors. A.5 shows that the results regarding the factors and variance decomposition are very similar to the benchmark case.

B Gibbs Sampling Algorithm

The empirical model is defined as:

$$\begin{pmatrix} T_{it} \\ P_{it} \end{pmatrix} = \begin{pmatrix} B_i^{W,T} & 0 \\ 0 & B_i^{W,P} \end{pmatrix} \begin{pmatrix} F_t^{W,T} \\ F_t^{W,P} \end{pmatrix} + \begin{pmatrix} B_i^{R,T} & 0 \\ 0 & B_i^{R,P} \end{pmatrix} \begin{pmatrix} F_t^{R,T} \\ F_t^{R,P} \end{pmatrix} + \begin{pmatrix} v_{it} \\ e_{it} \end{pmatrix} \quad (7)$$

where T denotes temperature series and P denotes precipitation series. The idiosyncratic components $u_{it} = \begin{pmatrix} v_{it} \\ e_{it} \end{pmatrix}$ are assumed to follow AR(1) processes:

$$u_{it} = \rho_i u_{it-1} + \Upsilon_{it} \quad (8)$$

The shocks Υ_{it} are assumed to have the following distribution:$\Upsilon_{it} \sim N(0, \sigma_{it})$. The variance σ_{it}^2 is allowed to evolve over time:

$$\ln \sigma_{it}^2 = \tilde{c}_i + \tilde{d}_i \ln \sigma_{it-1}^2 + g_i v_{it} \quad (9)$$

The world and regional factors are assumed to follow a VAR process:

$$Z_t = c + \sum_{j=1}^{P} b_j Z_{t-j} + E_t \quad (10)$$

where $\underbrace{Z_t}_{N\times 1} = \left(F_t^{W,J}, F_t^{R,J}\right)$ for $J = [T, P]$ The covariance matrix of E_t is assumed to be diagonal for the purpose of identification. Each element of E_t is distributed normally: $E_{kt} \sim N\left(0,\ h_{kt}\right)$ for $k = 1, .., N$. The stochastic volatilities h_{kt} evolve as random walks:

$$\ln h_{kt} = \bar{c_k} + \bar{D}_k \ln h_{kt-1} + d_k u_{kt} \tag{11}$$

B.1 Priors

We use the following prior distributions

1. The factor loadings are denoted by $b_i = [B_i^{W,J}, B_i^{R,J}]$ for for $J = [T, P]$. The prior is normal: $P(b_i) \sim N(\tilde{b_i}, \Sigma_b)$ where $\tilde{b_i}$ denotes principal component estimates of factor loadings and Σ_b is a diagonal matrix with diagonal elements equal to 0.1.

2. The prior for the persistence of the idiosyncratic components ρ_i is normal: $N(\rho_0, \Sigma_p)$ where $\rho_0 = 0.5$ and $\Sigma_p = 0.01$

3. The prior for the coefficients $\tilde{A}_i = [\tilde{c_i}, \tilde{d_i}]$ is normal with mean $A_0 = [0, 0.95]$ and variance Σ_A where Σ_A is a diagonal matrix with 0.1 on the main diagonal.

4. The prior for g_i is inverse Gamma with scale $g_0 = 0.001$ and degrees of freedom $T_0 = 1$

5. We use a Minnesota type prior (see Bańbura *et al.* (2010) for the coefficients of the VAR in equation 10 which are denoted by $\bar{\beta}$ in vectorised form. The tightness parameter is set to 0.1

6. The prior for $\bar{A}_k = [\bar{c_i}, \bar{d_i}]$ is normal with mean $\bar{A}_0 = [0, 0.95]$ and with variance $\bar{\Sigma}_A$, a diagonal matrix with diagonal elements equal to 0.1.

7. The prior for d_k is inverse Gamma with scale $d_0 = 0.001$ and degrees of freedom $T_{d,0} = 1$

The Gibbs sampling algorithm draws from the following conditional posterior distributions in each iteration (Ψ denotes all other parameters):

1. Factor loadings $G(b_i|\Psi)$. For each series y_{it} the model can be written as:

$$y_{it} = b_i z_t + u_{it} \tag{12}$$

$$u_{it} = \rho_i u_{it-1} + \Upsilon_{it} \tag{13}$$

$$var(\Upsilon_{it}) = \sigma_{it} \tag{14}$$

where $z_t = [F_t^{W,J}, F_t^{R,J}]$ for $J = T$ or $J = P$. A GLS transformation can be used to remove the autocorrelation and heteroscedasticity. Define $y_{it}^* = \frac{y_{it} - \rho y_{it-1}}{\sigma_{it}^{0.5}}$ and $x_{it}^* = \frac{z_{it} - \rho z_{it-1}}{\sigma_{it}^{0.5}}$. The conditional posterior is normal with variance $V = \left(\Sigma_b^{-1} + x_i^{*\prime} x_i^*\right)^{-1}$ and mean $M = V\left(\Sigma_b^{-1}\tilde{b}_i + x_i^{*\prime} y_i^*\right)$.

2. Persistence of idiosyncratic components $G(\rho_i|\Psi)$. Conditional on the remaining parameters, the idiosyncratic components can be written as:

$$u_{it} = \rho_i u_{it-1} + \Upsilon_{it} \tag{15}$$

$$var(\Upsilon_{it}) = \sigma_{it} \tag{16}$$

A GLS transformation can be used to remove heteroscedasticity. Define $y_{it}^* = \frac{u_{it}}{\sigma_{it}^{0.5}}$ and $x_{it}^* = \frac{u_{it-1}}{\sigma_{it}^{0.5}}$. The conditional posterior is normal with mean and variance defined as in Step 1 above.

3. Stochastic volatility of idiosyncratic components $G(\sigma_{it}|\Psi)$. Conditional on the remaining parameters, a non-linear state-space model applies to each idiosyncratic component:

$$u_{it} = \rho_i u_{it-1} + \Upsilon_{it} \tag{17}$$

$$var(\Upsilon_{it}) = \sigma_{it} \tag{18}$$

$$\ln \sigma_{it}^2 = \tilde{c}_i + \tilde{d}_i \ln \sigma_{it-1}^2 + g_i v_{it} \tag{19}$$

We draw σ_{it} from the conditional posterior using the particle Gibbs sampler with ancestor sampling introduced by Lindsten *et al.* (2014).

4. $G(g_i|\Psi)$. This conditional posterior is inverse Gamma with scale parameter $g_0 + \left(\ln \sigma_{it}^2 - \tilde{c}_i - \tilde{d}_i \ln \sigma_{it-1}^2\right)' \left(\ln \sigma_{it}^2 - \tilde{c}_i - \tilde{d}_i \ln \sigma_{it-1}^2\right)$ and degrees of freedom $T_i + T_0$ where T_i denotes the time-series for the ith cross-section.

5. $G(\tilde{A}_i|\Psi)$. The transition equation for the stochastic volatility is a linear regression model. Conditional on $ln\sigma_{it}^2, g_i$, the conditional posterior is normal. Let $y = ln\sigma_{it}^2$ and $x = [1, ln\sigma_{it-1}^2]$. Then the variance of the conditional posterior is defined as: $V = \left(\Sigma_A^{-1} + \frac{1}{g_i} x'x\right)^{-1}$ and mean $M = V\left(\Sigma_A^{-1} A_0 + \frac{1}{g_i} x'y\right)$

6. VAR coefficients $G(\bar{\beta}|\Psi)$. Conditional on the remaining parameters 10 is a VAR with heteroscedastic disturbances. As we assume that the covariance matrix of E_t is diagonal, one can draw from the conditional posterior of the coefficients equation by

equation. The conditional posterior is normal after a GLS transformation. Carriero *et al.* (2022) describe an efficient algorithm to implement this draw and we follow their approach.

7. Stochastic volatility $G(h_k|\Psi)$. The transition equations can be cast as a non-linear state-space system:

$$Z_t = c + \sum_{j=1}^{P} b_j Z_{t-j} + E_t \tag{20}$$

$$\ln h_{kt} = \bar{c_k} + \bar{D}_k \ln h_{kt-1} + d_k u_{kt} \tag{21}$$

   As in step 3, we employ a particle Gibbs sampler to draw h_{kt} from the conditional posterior distribution.

8. $G(d_k|\Psi)$. This step is identical to Step 4.

9. $G(\bar{A}_k|\Psi)$. This step is identical to Step 5.

Figure A.1: Contribution of the regional factor to temperature volatility

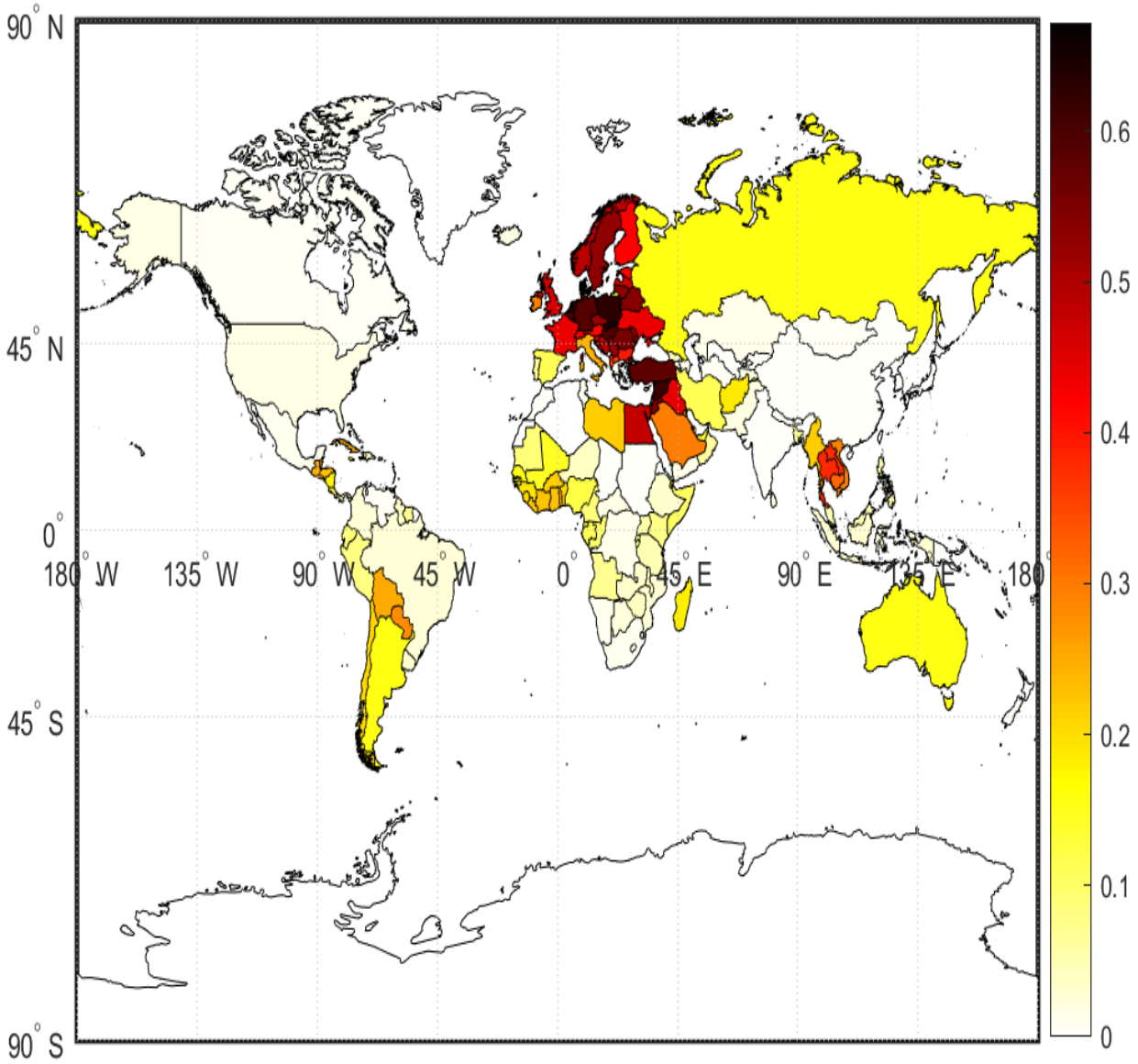

Darker colours the heat map indicates a larger contribution

Figure A.2: Contribution of the regional factor to precipitation volatility

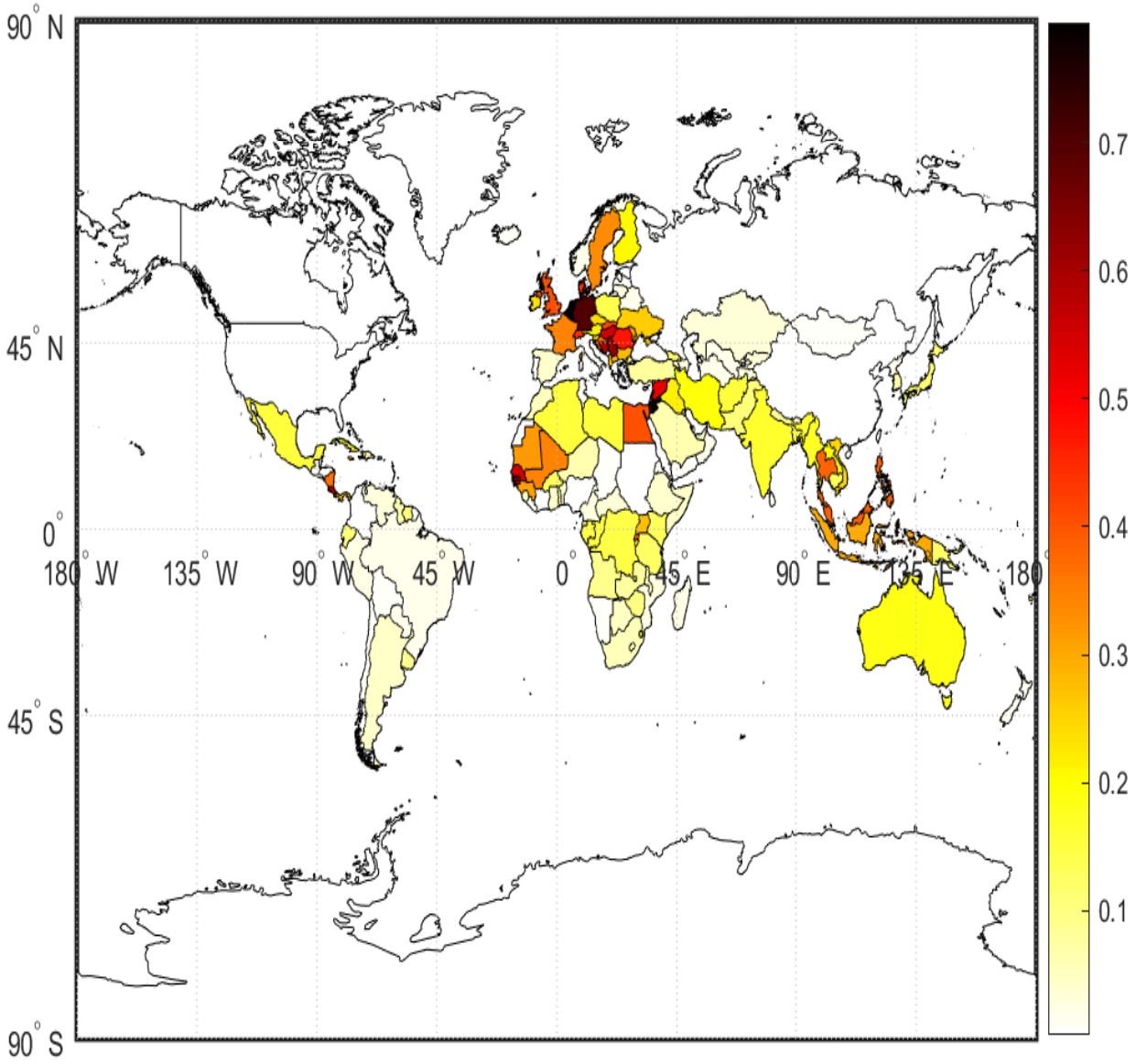

Darker colours the heat map indicates a larger contribution

Figure A.3: Robustness: Fat tails

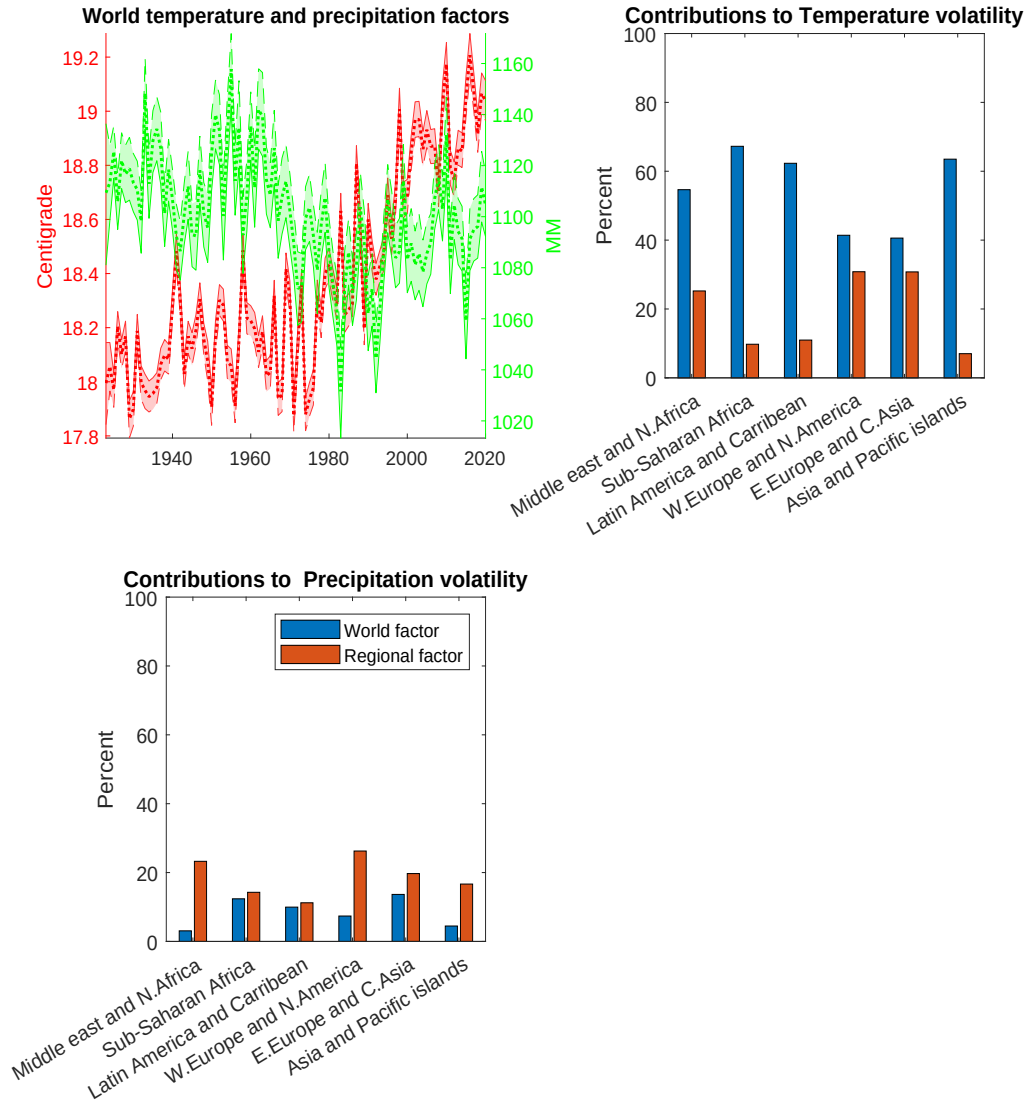

Figure A.4: Robustness: Two factors

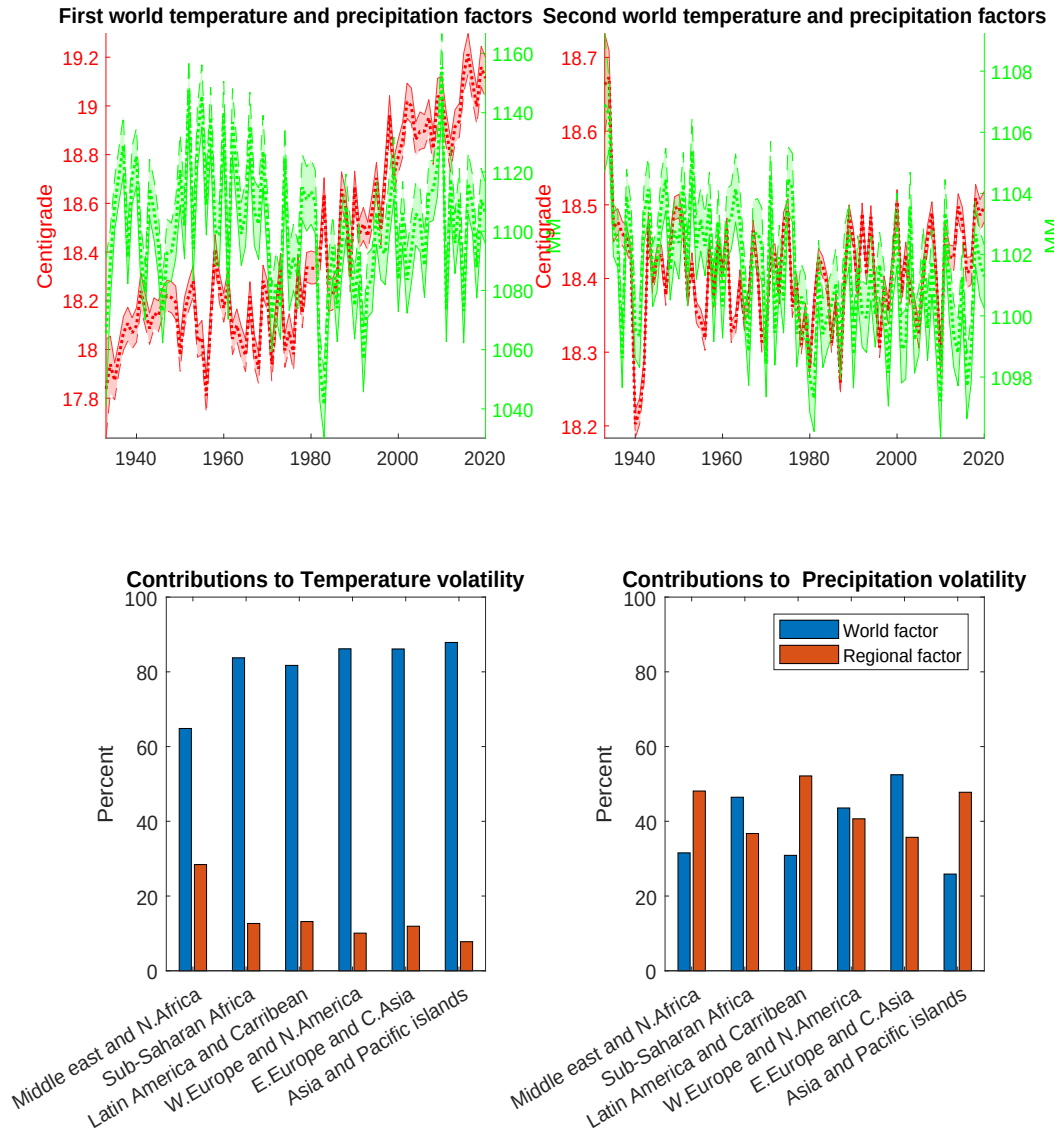

Figure A.5: Robustness: Longer lags